Lattice dynamics and phase transitions in $KAl(MoO_4)_2$, $RbAl(MoO_4)_2$ and $CsAl(MoO_4)_2$ layered crystals

2004 J. Phys.: Condens. Matter 16 3319

(http://iopscience.iop.org/0953-8984/16/20/003)

INSTITUTE OF PHYSICS PUBLISHING JOURNAL OF PHYSICS: CONDENSED MATTER

J. Phys.: Condens. Matter **16** (2004) 3319–3328 PII: S0953-8984(04)76122-6

Lattice dynamics and phase transitions in $KAl(MoO_4)_2$, $RbAl(MoO_4)_2$ and $CsAl(MoO_4)_2$ layered crystals

M Mączka[1], K Hermanowicz[1], P E Tomaszewski[1] and J Hanuza[1,2]

[1] Institute of Low Temperature and Structure Research, Polish Academy of Sciences, PO Box 1410, 50-950 Wrocław 2, Poland

[2] Department of Bioorganic Chemistry, Faculty of Industry and Economics, Wrocław University of Economics, 118/120 Komandorska Street, 53-345 Wrocław, Poland

Received 9 February 2004, in final form 6 April 2004
Published 7 May 2004
Online at stacks.iop.org/JPhysCM/16/3319
DOI: 10.1088/0953-8984/16/20/003

Abstract

Raman and IR studies of $KAl(MoO_4)_2$, $RbAl(MoO_4)_2$ and $CsAl(MoO_4)_2$ are reported. The assignments of modes are given on the basis of lattice dynamics calculations. The temperature dependence of the $KAl(MoO_4)_2$ vibrational modes shows that this compound exhibits a second-order phase transition around 90 K from the $P\bar{3}m1$ to most probably a monoclinic and ferroelastic phase.

1. Introduction

$KAl(MoO_4)_2$, $RbAl(MoO_4)_2$ and $CsAl(MoO_4)_2$ belong to the large crystal family of layered double molybdates and tungstates with the general formula $M^IM^{III}(M^{VI}O_4)_2$, where M^I = Na, K, Rb, Cs, M^{III} = Al, Sc, In, Cr and M^{VI} = Mo, W. These compounds have been of considerable interest since many of them exhibit a sequence of ferroelastic phase transitions induced by rigid rotations of MoO_4^{2-} tetrahedra [1–3]. Rigid rotation of tetrahedra gives rise to ferroelastic phase transitions in many molybdates, phosphates and silicates—for example, in rare-earth pentaphosphates ReP_5O_{14} (with Re = La to Tb) [4] and $M_2^{III}(MoO_4)_3$ molybdates (with M^{III} = Gd, Tb, Sc, In) [5, 6]. Our recent studies showed also that alkali metal–aluminium molybdates doped with chromium (III) ions exhibit efficient luminescence and, therefore, are promising hosts for laser applications [7, 8]. Since the emission spectra exhibit the presence of many vibronic transitions, understanding the emission behaviour of these crystals requires knowledge of the phonon properties. In our previous papers we have established wavenumbers and symmetries of IR and Raman active modes of $KAl(MoO_4)_2$ [9, 10]. The tentative assignment of modes was also proposed. However, this assignment was based only on experimental results. The present paper gives much more precise assignments of modes

obtained with the use of lattice dynamics calculations. This paper also gives information on vibrational properties of $RbAl(MoO_4)_2$ and $CsAl(MoO_4)_2$, not studied previously.

It is also worth noting that a previously reported electron spin resonance (ESR) study showed that $KAl(MoO_4)_2$ exhibits two phase transitions at around 80 and 50 K [11]. We decided, therefore, to perform temperature-dependent Raman and IR studies on $KAl(MoO_4)_2$ in order to obtain information on the nature of the phase transition. The results obtained show that the 80 K transition (observed in the present study around 90 K) leads to splitting of some vibrational modes. This behaviour is very similar to the behaviour of other trigonal molybdates and tungstates and, therefore, we may conclude that the $P\bar{3}m1$ phase of $KAl(MoO_4)_2$ transforms below 90 K to a ferroelastic phase, most probably of $C2/c$ symmetry.

2. Experiment

The growth of single crystals was described previously [9, 10].

Polycrystalline infrared spectra were measured for the ground crystals in a KBr suspension, with a Perkin-Elmer 2000 FT-IR spectrometer, for the 1500–400 cm^{-1} region and in Nujol suspension for the 500–30 cm^{-1} region. FT Raman spectra were measured using a BRUKER 110/S spectrometer with YAG:Nd^{3+} excitation. Temperature-dependent studies of IR and Raman spectra were performed using a helium-flow Oxford cryostat. Both IR and Raman spectra were recorded with a spectral resolution of 2 cm^{-1}.

3. Results and discussion

3.1. The model used in the lattice dynamics calculations

The calculations of wavenumbers and displacement vectors were performed on the basis of a partially ionic model described previously [12]. The atomic positions used in the calculations were taken from [13] (for $CsAl(MoO_4)_2$) and from our recent x-ray studies of $KAl(MoO_4)_2$ and $RbAl(MoO_4)_2$ (the papers are in preparation). The following potential between the ith and jth atoms was used in these calculations:

$$U_{ij}(r_{ij}) = z_i z_j e^2/r_{ij} + (b_i + b_j)\exp[(a_i + a_j - r_{ij})/(b_i + b_j)] - c_i c_j/r_{ij}^6 + D_{ji}(\exp[-2\beta_{ij}(r_{ij} - r_{ij}^*)] - 2\exp[-\beta_{ij}(r_{ij} - r_{ij}^*)]).$$

This potential consists of a Coulomb interaction (first term), Born–Mayer type repulsive interaction (second term), van der Waals attractive interaction (third term) and Morse potential contribution (last term). z_i and z_j are the effective charges of the ions i and j, respectively, separated by distance r_{ij}. The parameters a_i, a_j and b_i, b_j reflect the ionic radius and ionic stiffness, respectively. We consider covalency for the Mo–O bonds only. The initial values of the parameters for oxygen, molybdenum and potassium ions were taken from [12] and [14]. The values of the parameter b for the rubidium, caesium and aluminium ions were assumed to be the same as that for K^+. Since the parameters a are correlated with the ionic radii, their initial values were obtained for the rubidium, caesium and aluminium ions using the values for the potassium and molybdenum ions, i.e. they were calculated using the following expressions: $a_{Rb} = a_K r_{Rb}/r_K$, $a_{Cs} = a_K r_{Cs}/r_K$ and $a_{Al} = a_{Mo} r_{Al}/r_{Mo}$ where r denotes the ionic radius. Since the application of these initial parameters during the calculations resulted in the appearance of some negative frequencies, it was necessary to change the initial parameters for Mo as well as the parameters a for oxygen and aluminium ions in order to obtain only positive frequencies and the best agreement between the observed and calculated wavenumbers. The final parameters used in the present calculations are listed in table 1.

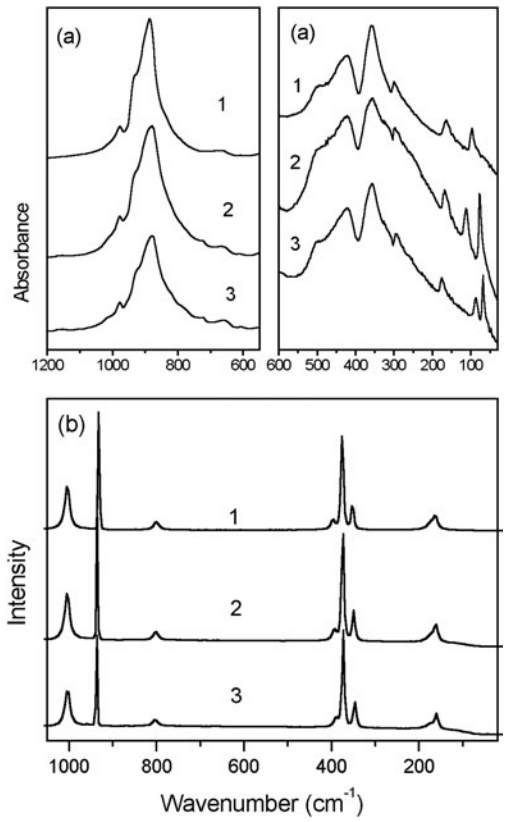

Figure 1. Polycrystalline IR (a) and Raman (b) spectra of $KAl(MoO_4)_2$ (1), $RbAl(MoO_4)_2$ (2) and $CsAl(MoO_4)_2$ (3).

Table 1. Potential parameters used for the lattice dynamics calculations.

ith ion	z_i (e)	a_i (Å)	b_i (Å)	C (kcal$^{1/2}$ Å^3 mol$^{-1/2}$)
Mo	2.85	0.938	0.09	0
O	−1.05	1.882	0.16	20
Al	2.1	0.998	0.09	0
K	0.6	1.758	0.09	15
Rb	0.6	1.874	0.09	20
Cs	0.6	1.963	0.09	25
Ion pair	D_{ji} (kcal mol^{-1})	β_{ij} (Å)	r_{ij}^* (Å)	
Mo–O	26.0	2.2	1.95	

3.2. Vibrational properties at ambient temperature

There are 36 ($\mathbf{k} = 0$) vibrational modes for the trigonal $P\bar{3}m1$ structure. These modes may be subdivided into $A_{2u} + E_u$ acoustic modes, $2A_{1g} + E_g + 2A_{2u} + E_u$ stretching modes, $A_{1g} + 2E_g + A_{2u} + 2E_u$ bending modes, $A_{1g} + E_g + 2A_{2u} + 2E_u$ translational modes and $A_{2g} + E_g + A_{1u} + E_u$ librational modes.

The measured Raman and IR spectra are presented in figure 1 and the measured wavenumbers are listed in table 2. As can be seen, the Raman active modes of $KAl(MoO_4)_2$,

Table 2. Observed and calculated wavenumbers (in cm^{-1}) for Raman (A_{1g} and E_g) and IR (A_{2u} and E_u) modes of $KAl(MoO_4)_2$, $RbAl(MoO_4)_2$ and $CsAl(MoO_4)_2$ together with proposed assignments. For the IR active mode the LO wavenumbers are given in parentheses. ν_1, ν_3, ν_2 and ν_4 denote symmetric stretching, asymmetric stretching, symmetric bending and asymmetric bending vibrations of MoO_4^{2-} units, respectively. $T'(Al^{3+})$, $T'(MoO_4)$, $T'(M^+)$ and $L(MoO_4)$ denote translations of Al^{3+}, MoO_4^{2-} and alkali metal ions and librations of MoO_4^{2-} ions, respectively. '*' are used to show the coupling of modes.

$KAl(MoO_4)_2$		$RbAl(MoO_4)_2$		$CsAl(MoO_4)_2$			
Observed	Calculated	Observed	Calculated	Observed	Calculated	Symmetry	Assignment
1003	982	1004	1010	1003	1004	A_{1g}	ν_1
931	927	936	943	937	930	A_{1g}	ν_3
802	802	803	835	803	827	E_g	ν_3
395	595	394	580	390	567	A_{1g}	ν_4
375	497	374	498	373	486	E_g	ν_4
352	336	349	322	346	310	E_g	ν_2
173	176	170	162	171	159	A_{1g}	$T'(MoO_4)$
164	203	162	183	160	179	E_g	$T'(MoO_4)$*$L(MoO_4)$
—	135	—	118	—	90	E_g	$L(MoO_4)$*$T'(MoO_4)$
980	949 (972)	978	963 (978)	979	950 (957)	A_{2u}	ν_1
932	914 (924)	926	932 (949)	920	915 (939)	A_{2u}	ν_3
888	837 (870)	881	871 (902)	881	865 (893)	E_u	ν_3
505	474 (627)	504	465 (612)	504	466 (603)	A_{2u}	ν_4*$T'(Al^{3+})$
428	463 (594)	426	455 (585)	421	450 (578)	E_u	ν_4*$T'(Al^{3+})$*$T'(MoO_4)$
359	394 (407)	362	377 (383)	364	366 (367)	E_u	ν_2*$T'(Al^{3+})$*$T'(MoO_4)$
303	305 (308)	299	305 (312)	295	307 (316)	E_u	ν_2*$T'(Al^{3+})$*$T'(MoO_4)$
—	356 (358)	—	268 (270)	—	237 (241)	A_{2u}	$T'(Al^{3+})$*$T'(MoO_4)$
167	173 (195)	171	163 (206)	175	186 (222)	E_u	$L(MoO_4)$
174	213 (216)	115	178 (179)	90	135 (136)	A_{2u}	$T'(M^+)$
99	92 (161)	77	92 (113)	69	80 (90)	E_u	$T'(M^+)$

$CsAl(MoO_4)_2$ and $RbAl(MoO_4)_2$ have very similar wavenumbers. We may, therefore, assign the observed modes to respective symmetries on the basis of our previous Raman study of $KAl(MoO_4)_2$ [10]. The three modes above 800 cm^{-1} can be unambiguously assigned to the stretching modes. It is worth noticing that the lattice dynamics calculations show pronounced difference between the 930 cm^{-1} stretching mode and the stretching modes observed around 800 and 1000 cm^{-1}. The first mode exhibits very large stretches of the Mo–O1 bonds which are parallel to the *c*-axis whereas the two other modes involve large motions of the remaining oxygen atoms, which have short distances to Al^{3+} ions (denoted in this paper as O2). Since the O1 oxygen atoms do not interact with the Al^{3+} ions and interact very weakly with the alkali metal ions, the corresponding mode around 930 cm^{-1} is characterized by very weak anharmonicity, as evidenced through the very small bandwidth of this mode. On the other hand, the remaining modes give rise to broad Raman bands. The unusual feature of the molybdates and tungstates, crystallizing in the $P\bar{3}m1$ structure, is that the narrow mode is always observed around 930 cm^{-1}, whereas the remaining stretching modes are observed in a much broader wavenumber range, i.e. 780–810 and 950–1010 cm^{-1} [10, 15, 16].

The three predicted bending modes are observed in the 340–400 cm^{-1} range. Our lattice dynamics calculations suggest that the E_g modes around 370 and 350 cm^{-1} may be assigned to asymmetric bending modes and symmetric bending modes, respectively.

As far as the Raman active lattice modes are concerned, the Al^{3+} and K^+ ions must necessarily be at rest since they are situated at inversion centres. The A_{1g} and E_g translational

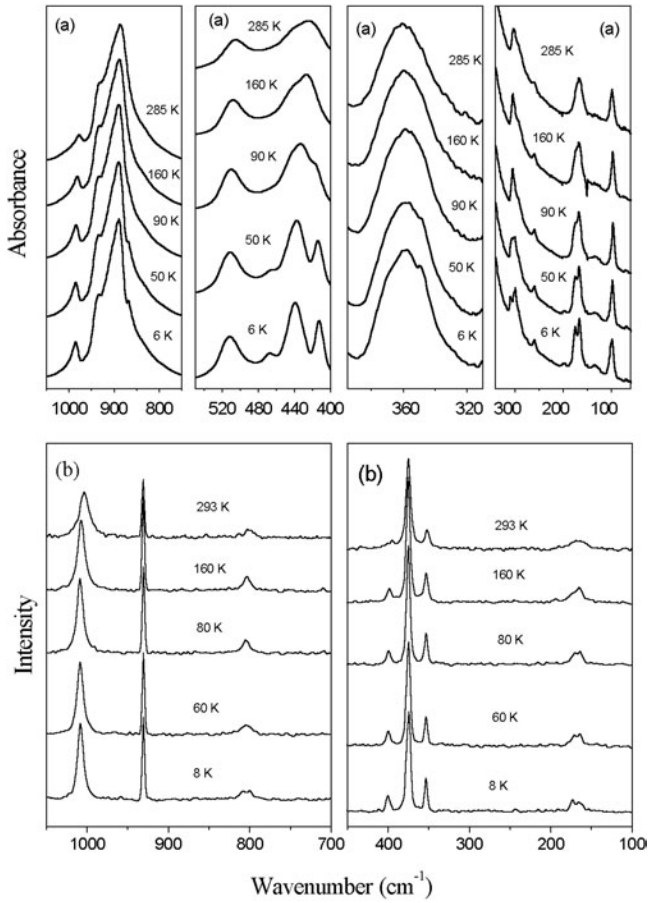

Figure 2. Temperature dependences of IR (a) and Raman (b) spectra of $KAl(MoO_4)_2$ at selected temperatures.

modes describe, therefore, translational motions of the MoO_4^{2-} ions. The A_{1g} mode is located at 175–170 cm^{-1}. As far as E_g modes are concerned, we previously assigned the 164 cm^{-1} mode of $KAl(MoO_4)_2$ to the translations of MoO_4^{2-} ions and the 64 cm^{-1} band to the librational mode [10]. The lattice dynamics calculations performed show, however, that the E_g modes may couple and, therefore, that they should rather be assigned as mixed modes. According to the calculations, the contribution of translational motions is larger for the 175–170 cm^{-1} modes and librational motions for the $\sim$60 cm^{-1} mode.

In the case of IR active modes, our previous study unambiguously showed that the A_{2u} stretching modes are observed at 976 and 932 cm^{-1} for $KAl(MoO_4)_2$ and the E_u stretching mode at 880 cm^{-1} [9]. The lattice dynamics calculations confirm this assignment (see table 2). The assignment of the low wavenumber modes is less clear and we may expect to observe significant mixing between librational, translational and bending modes of the same symmetry. The comparison of the spectra measured for K, Rb and Cs molybdates reveals that these spectra have similar contours in the 290–500 cm^{-1} region. This result shows that translational motions of alkali metal ions do not contribute significantly to these modes. The lattice dynamics calculations show that these modes should be assigned to the

bending modes of the MoO_4^{2-} ions coupled with translational motions of aluminium ions and molybdate tetrahedra. These calculations overestimate, however, the contribution of the alkali metal motions to one of these modes, especially for the potassium molybdate and as a result incorrectly predict a strong wavenumber dependence on the alkali metal ion mass of the lower wavenumber A_{2u} mode (see table 2). It is worth noting that the IR spectra show the presence of four modes in the 290–500 cm^{-1} region whereas five modes should be observed. One of the modes is not observed in the IR spectra since it is most probably overlapped with another broad band. The missing mode is most probably located around 280 cm^{-1} since our recent luminescence study of these crystals revealed the presence of a relatively strong vibronic band around 280–286 cm^{-1} [7, 8].

It should be noted that the crystal field splittings of the ν_2, ν_3 and ν_4 internal modes are very large for this class of compounds (see table 2). Since it has been previously shown for scheelite tungstates that the splittings arise from interionic forces [17], the observed large splittings indicate the presence of strong interactions between MoO_4^{2-} tetrahedra in the trigonal molybdates studied.

Only three IR active lattice modes (the librational mode of E_u symmetry and translational modes of A_{2u} and E_u symmetry) should be observed for the crystals studied. These modes are observed below 200 cm^{-1} (see figure 1). The IR mode observed around 170 cm^{-1} shows slight wavenumber increase with increasing ionic radius of the alkali metal ion and it can be, therefore, assigned to the E_u libration of the MoO_4^{2-} ions. The two remaining modes show very clear wavenumber decrease with increasing mass of the alkali metal ion (see table 2). This result suggests that they should be assigned to translational motions of the alkali metal ions. The lattice dynamics calculations show that the higher wavenumber mode has A_{2u} and the lower wavenumber mode E_u symmetry. These calculations predict also that there should be significant coupling between the librational and translational modes of E_u symmetry. The contribution of translational motions of the alkali metal ions to the 170 cm^{-1} mode is predicted to decrease very significantly in the order K > Rb > Cs whereas the opposite trend is predicted for the mode observed below 100 cm^{-1}.

3.3. Temperature dependence of IR and Raman modes of $KAl(MoO_4)_2$

The temperature-dependent studies show the presence of splitting at low temperatures of the 802 cm^{-1} Raman active mode and the 888, 428, 359 and 303 cm^{-1} IR active modes (see figures 2 and 3). The observed splitting of these doubly degenerate modes indicates that symmetry is lowered. Since it is known that many trigonal molybdates and tungstates exhibit ferroelastic phase transitions into $C2/c$, $C2/m$ or C_i structure [1], it is very likely that the low temperature phase of $KAl(MoO_4)_2$ is also monoclinic or triclinic. The previous EPR studies suggested that the phase transition around 80 K occurs most probably to a monoclinic phase [11].

It has previously been shown that the analysis of the asymmetric stretching mode splitting may give information on the temperature dependence of the order parameter [15]. Unfortunately, this type of analysis is not reliable in the case of $KAl(MoO_4)_2$ since the splitting of the E_g mode is small and its intensity weak. The information on the temperature dependence of the order parameter can, however, also be obtained from an analysis of band intensity changes induced by a phase transition [18–22]. In our case the most suitable band for this kind of analysis is the 416 cm^{-1} IR band since it shows large and continuous intensity changes and is relatively well separated from the other bands. The dependence of the intensity of this band versus temperature is presented in figure 4(a). This figure shows that near 0 K the slope of the experimental points is near zero. This kind of behaviour is usually observed when

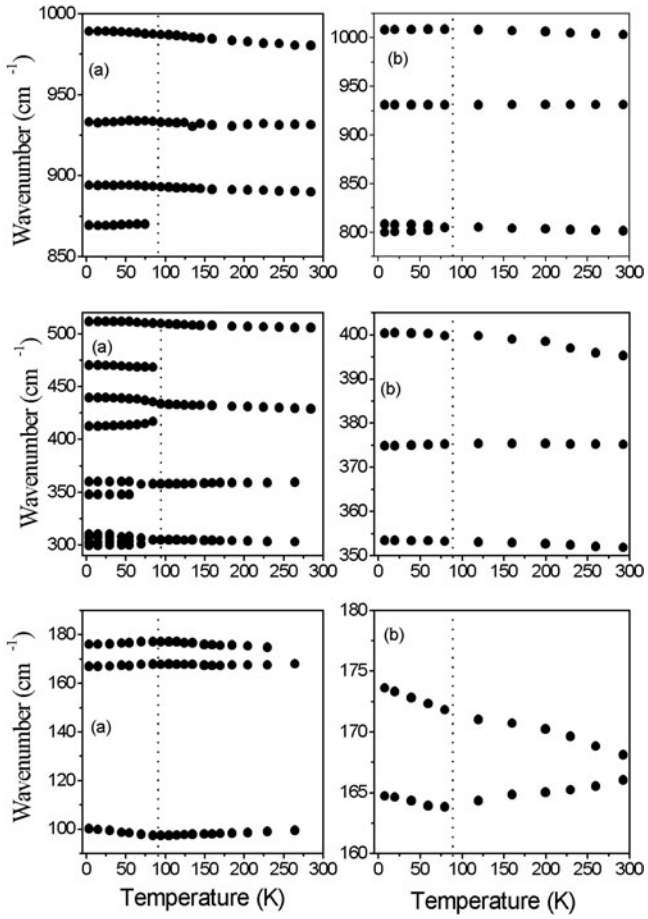

Figure 3. IR (a) and Raman (b) wavenumbers versus temperature for $KAl(MoO_4)_2$. The dotted vertical line indicates the phase transition temperature.

the phase transition is induced by instability of a soft mode and it is explained by soft mode frequency saturation since each thermodynamic parameter should reach 0 K with a slope equal to zero [23]. It has previously been shown that if the phase transition is second order, the order parameter $\eta(T)$, or any other parameter proportional to it, may be well approximated by the following function [24]:

$$\eta(T) = \eta(0)B_s\left[\frac{3s}{s+1}\frac{\eta(T)T_1}{\eta(0)T}\right] \tag{1}$$

where B_s is the Brillouin function for spin s. The result of experimental data fitting to this formula is shown in figure 4(a) (we assume that the intensity $I(T)$ of the 416 cm^{-1} IR band is proportional to the order parameter). The adjustable parameters are $I(0)$, T_1 and s. We see a very good fit to $I(T)$ for $s = 1$, $I(0) = 7.85$ and $T_1 = 93$ K. This result shows that the phase transition in $KAl(MoO_4)_2$ is of second order and can be well described by the mean field theory with the critical exponent $\beta = 0.5$. It is worth noting that the phase transition temperature (T_1) obtained in this way is about 10 K higher than that suggested by the ESR studies. The origin of this discrepancy is not clear.

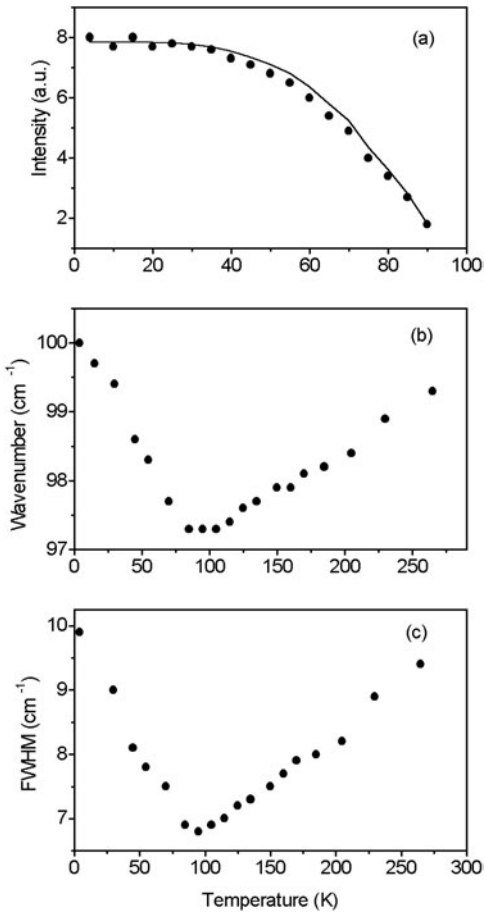

Figure 4. The intensity of the ∼416 cm^{-1} IR band (a), as well as the wavenumber (b) and full width at half-maximum (c), for the ∼99 cm^{-1} IR mode versus temperature. The solid curve in the plot (a) was obtained from the fitting of the intensity to expression (1).

Another characteristic feature of this crystal is the temperature behaviour of the E_u librational mode observed around 99 cm^{-1}. The energy of this mode exhibits an anomalous decrease with temperature lowering down to ∼90 K (see figure 4(b)). Further temperature lowering leads to wavenumber increase. The linear fitting of the data above and below 90 K shows that the two lines intersect at 89.6±1.8 K, i.e. the energy of this mode exhibits a minimum at the phase transition temperature. Since it is known that the phase transition in this class of compounds is induced by softening of some modes, the observed behaviour of the E_u modes may be due to the presence of some coupling between this mode and a soft mode. The analysis of the damping (Γ) of the librational mode discussed shows that its temperature dependence is very similar to the temperature dependence of the energy, i.e. it shows a minimum at the phase transition (see figure 4(c)). The intersection of the straight lines, obtained from a linear fitting of the data points, gives $T_1 = 90.1 \pm 1.6$ K. The anomalous increase of the damping below 90 K can be most probably attributed to the appearance of a small, unresolved splitting of this degenerate mode below T_1. This splitting should increase with decreasing temperature leading to anomalous increase of the damping below 90 K.

It is worth noting that our studies show, in addition to the observed E_u mode splitting, the appearance of a weak IR band around 470 cm^{-1} below 90 K. Since the mode around 500 cm^{-1} is not degenerate (A_{2u}), the appearance of this weak band cannot be attributed to the splitting of the 500 cm^{-1} mode. It could be attributed to the splitting of a missing doubly degenerate mode, overlapped with the E_u mode around 430 cm^{-1}. However, since the group theory predicts the presence of three E_u and two A_{2u} modes in this region, the assignment of the 430 cm^{-1} band to two overlapping E_u modes would mean that either the 353 or 303 cm^{-1} mode has A_{2u} symmetry. This seems, however, to be inconsistent with the observation of a clear splitting for these modes below 90 K. We conclude, therefore, that the origin of the 470 cm^{-1} mode cannot be clearly explained on the basis of the present studies.

The studies performed show also that many stretching and bending modes show significantly different temperature dependences in the trigonal and low temperature phases. In particular, the 980, 888, 505 cm^{-1} IR active and 1003, 395, 375, 352 cm^{-1} Raman active modes show wavenumber increase with temperature lowering in the trigonal phase but practically no wavenumber change in the low temperature phase. This behaviour can most probably be attributed to the presence of an additional compression mechanism available below 90 K; whereas in the trigonal structure the MoO_4^{2-} tetrahedra cannot rotate (they are fixed by symmetry), in the monoclinic or triclinic structure they can gradually tilt about the twofold axes [2, 3, 10].

Finally, the studies performed show that the IR band around 300 cm^{-1} exhibits a splitting into four components at low temperatures. Such splitting could be attributed to the presence of a second phase transition at 50 K, reported in ESR studies. However, the temperature behaviour of the split components suggests that this splitting is already observed near 90 K but it is small and, therefore, not clearly visible. We suppose, therefore, that the observed splitting (into four components) can be explained as a result of E_u mode splitting into two $A_u + B_u$ Davydov doublets in the monoclinic phase, rather than the presence of another phase transition into a triclinic phase. The remaining IR and Raman modes do not show any peculiarities which could indicate the presence of the 50 K phase transition. This result shows that the 50 K transition has a very small effect on the MoO_4^{2-} unit.

4. Conclusions

The lattice dynamics calculations predict well the wavenumbers of the majority of modes. However, they overestimate the contribution of alkali metal ion motions to a few modes, especially for the potassium derivative. These calculations explain the unusual behaviour of the 930 cm^{-1} stretching mode which is observed at nearly the same wavenumber for all molybdates and tungstates crystallizing in the $P\bar{3}m1$ structure, exhibits a very small bandwidth (<3 cm^{-1}) and shows almost no temperature dependence in bandwidth or energy. These features, indicating very small anharmonicity, are due to this mode involving large motions of the O1 oxygen atoms only.

The temperature dependence of the vibrational modes indicates that $KAl(MoO_4)_2$ exhibits a ferroelastic phase transition around 90 K to a monoclinic structure. The second, previously reported 50 K phase transition does not lead to any clearly visible changes in the vibrational spectra. Finally, we conclude that $KAl(MoO_4)_2$ should be added to the group of trigonal molybdates and tungstates exhibiting a sequence of ferroelastic phase transitions.

Acknowledgment

This work was supported by the Polish Committee for Scientific Research, grant No 7 TO9A 020 21.

References

[1] Otko A I, Nesterenko N M and Povstyanyi L V 1978 *Phys. Status Solidi* a **46** 577
[2] Otko A I, Nesterenko N M and Zvyagin A I 1979 *Izv. Akad. Nauk SSSR Ser. Fiz.* **43** 1675
[3] Nesterenko N M, Fomin V I and Kutko V I 1982 *Fiz. Nizk. Temp.* **8** 862
[4] Errandonea G 1980 *Phys. Rev.* B **21** 5221
[5] Yao W, Cummins H Z and Bruce R H 1981 *Phys. Rev.* B. **24** 424
[6] Sleight A W and Brixner L H 1973 *J. Solid State Chem.* **7** 172
[7] Hermanowicz K, Maczka M, Deren P J, Hanuza J, Stręk W and Drulis H 2001 *J. Lumin.* **92** 151
[8] Hermanowicz K 2004 *J. Lumin.* at press
[9] Maczka M, Hanuza J, Lutz E T G and van der Maas J H 1999 *J. Solid State Chem.* **145** 751
[10] Maczka M, Kojima S and Hanuza J 1999 *J. Raman Spectrosc.* **30** 339
[11] Hermanowicz K 2002 *J. Alloys Compounds* **341** 179
[12] Nozaki R, Kondo J N, Hirose C, Domen K, Wada A and Morioka Y 2001 *J. Phys. Chem.* B **105** 7950
[13] Tomaszewski P E, Pietraszko A, Maczka M and Hanuza J 2002 *Acta Crystallogr.* E **58** i119
[14] Saraiva G D, Maczka M, Freire P T C, Mendes Filho J, Melo F E A, Hanuza J, Morioka Y and Souza Filho A G 2003 *Phys. Rev.* B **67** 224108
[15] Maczka M, Kojima S and Hanuza J 1999 *J. Phys. Soc. Japan* **68** 1948
[16] Maczka M 1996 *J. Solid State Inorg. Chem.* **33** 783
[17] Scott J F 1968 *J. Chem. Phys.* **49** 98
[18] Petzelt J and Dvorak V 1976 *J. Phys. C: Solid State Phys.* **9** 1571
[19] Fleury P A 1972 *Comment. Solid State Phys.* **4** 167
[20] Scott J F and Chen T 1991 *Phase Transit.* B **32** 235
[21] Chen T and Scott J F 1990 *J. Raman Spectrosc.* **21** 761
[22] Chen T and Scott J F 1989 *Phys. Rev.* B **40** 8978
[23] Girard A, Delugeard Y, Ecolivet C and Cailleau H 1982 *J. Phys. C: Solid State Phys.* **15** 2127
[24] Kozlov G V, Volkov A A, Scott J F, Feldkamp G E and Petzelt J 1983 *Phys. Rev.* B **28** 255